PNAS
www.pnas.org

Supplementary Information for

Evolution and diversification of the plant gibberellin receptor GID1

Hideki Yoshida, Eiichi Tanimoto, Takaaki Hirai, Yohei Miyanoiri, Rie Mitani, Mayuko Kawamura, Mitsuhiro Takeda, Sayaka Takehara, Ko Hirano, Masatsune Kainosho, Takashi Akagi, Makoto Matsuoka, and Miyako Ueguchi-Tanaka

Makoto Matsuoka
Email: makoto@agr.nagoya-u.ac.jp
Miyako Ueguchi-Tanaka
Email: mueguchi@nuagr1.agr.nagoya-u.ac.jp

This PDF file includes:

Figs. S1 to S19
Tables S1 to S3
Captions for databases S1 to S4

Other supplementary materials for this manuscript include the following:

Datasets S1 to S4

www.pnas.org/cgi/doi/10.1073/pnas.1806040115

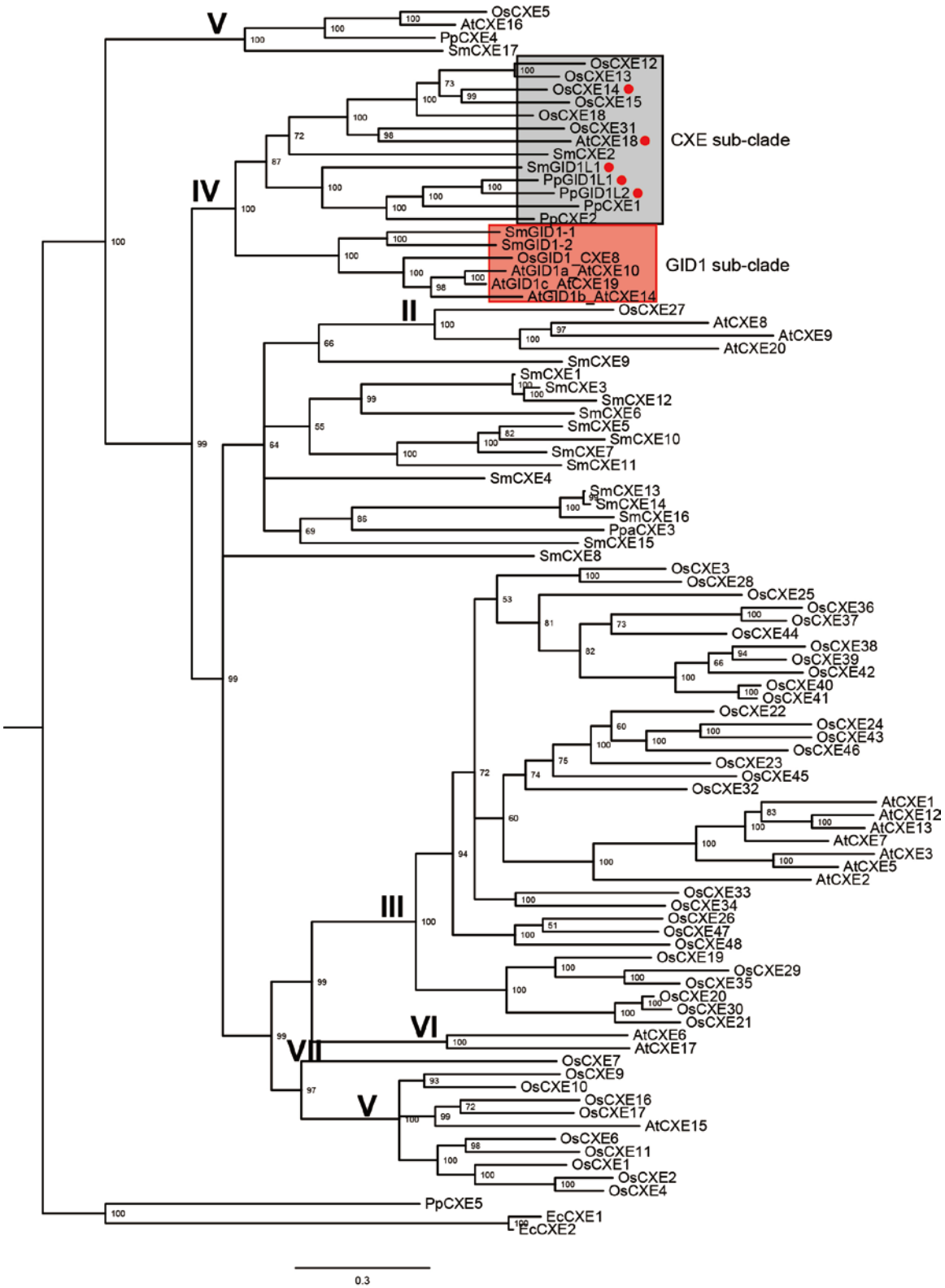
V
OsCXE5
AtCXE16
PpCXE4
SmCXE17
OsCXE12
OsCXE13
OsCXE14
OsCXE15
OsCXE18
OsCXE31
AtCXE18
SmCXE2
SmGID1L1
PpGID1L1
PpGID1L2
PpCXE1
PpCXE2
CXE sub-clade
IV
SmGID1-1
SmGID1-2
OsGID1_CXE8
AtGID1a_AtCXE10
AtGID1c_AtCXE19
AtGID1b_AtCXE14
GID1 sub-clade
II
OsCXE27
AtCXE8
AtCXE9
AtCXE20
SmCXE9
SmCXE1
SmCXE3
SmCXE12
SmCXE6
SmCXE5
SmCXE10
SmCXE7
SmCXE11
SmCXE4
SmCXE13
SmCXE14
SmCXE16
PpaCXE3
SmCXE15
SmCXE8
OsCXE3
OsCXE28
OsCXE25
OsCXE36
OsCXE37
OsCXE44
OsCXE38
OsCXE39
OsCXE42
OsCXE40
OsCXE41
OsCXE22
OsCXE24
OsCXE43
OsCXE46
OsCXE23
OsCXE45
OsCXE32
AtCXE1
AtCXE12
AtCXE13
AtCXE7
AtCXE3
AtCXE5
AtCXE2
III
OsCXE33
OsCXE34
OsCXE26
OsCXE47
OsCXE48
OsCXE19
OsCXE29
OsCXE35
OsCXE20
OsCXE30
OsCXE21
VI
AtCXE6
AtCXE17
VII
OsCXE7
OsCXE9
OsCXE10
V
OsCXE16
OsCXE17
AtCXE15
OsCXE6
OsCXE11
OsCXE1
OsCXE2
OsCXE4
PpCXE5
EcCXE1
EcCXE2
0.3

Fig. S1. Phylogenetic analysis of CXEs including GID1s in *A. thaliana* (At), rice (Os), *S. moellendorffii* (Sm), and *P. patens* (Pp), by Bayesian phylogenetic analysis based on the alignment presented in *SI Appendix*, Dataset S1. Branch nodes show posterior probability, and the horizontal branch lengths are proportional to the estimated number of amino acid substitutions per residue. The seven clades reported by Marshall et al. (17) are labeled by roman numerals. GID1s in red box and GID1-like CXEs in grey boxes are grouped into clade IV. The CXEs and GID1-likes (GID1L), marked by red dots, were used for further analysis. Bacterial CXEs, WP_061301181.1 (*E. coli* CXE1; EcCXE1) and WP_060616723.1 (EcCXE2), were used as out-groups.

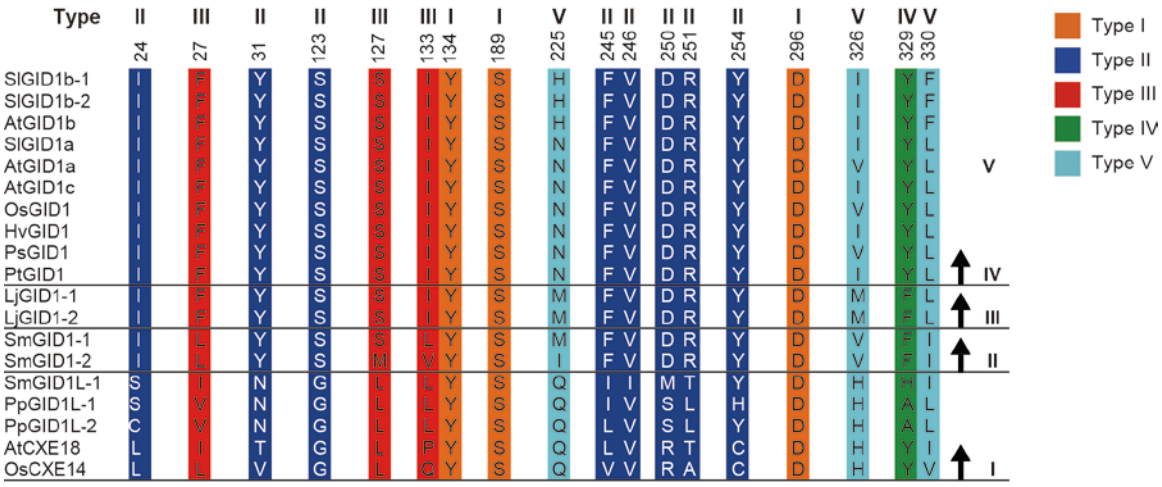

Fig. S2. Amino acid alignment of OsGID1, which interacts with GA_4. An alignment of entire amino acid sequences is presented in *SI Appendix*, Dataset S1. The alignment includes monocot GID1s from rice (Os) and barley (Hv); eudicot GID1s from *A. thaliana* (At) and tomato (Sl); gymnosperm GID1s from *Picea sitchenesis* (Ps), and *Pinus taeda* (Pt); fern GID1s from *L. japonica* (Lj); lycophyte GID1s from *S. moellendorffii* (Sm); and GID1-like CXEs from *P. patents* (PpGID1L-1 and PpGID1L-2), *S. moellendorffii* (SmGID1L-1), AtCXE18, and OsCXE14.

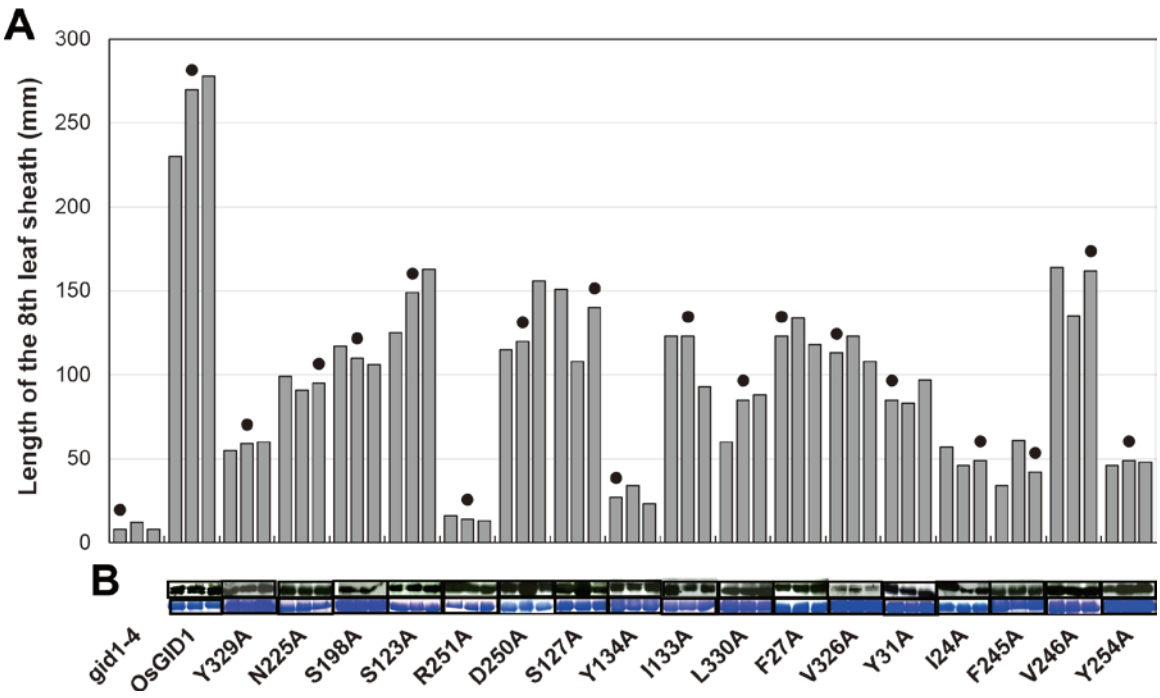

Fig. S3. Effect of replacement of GA_4-interacting amino acids with Ala on the OsGID1 activity (*A*) Length of the 8th leaf sheath of three independent *gid1* plants overexpressing the indicated mOsGID1s. We used plants having nearly the same amount of GID1 protein (marked with dots). (*B*) Western blot analysis with αOsGID1-antibody to confirm that the plants expressed a similar amount of mOsGID1 (upper panel). Lower panel shows the loading control.

Fig. S4. Ala or Ser substitution of six non-polar amino acids abrogates rescue of *gid1* dwarfism. (*A*) *gid1* expressing the wild type OsGID1. (*B* and *C*) mOsGID1 replaced with Ala (*B*) or Ser (*C*). The six replaced residues are indicated in red in *SI Appendix*, Dataset S1. Scale bars indicate 5 cm.

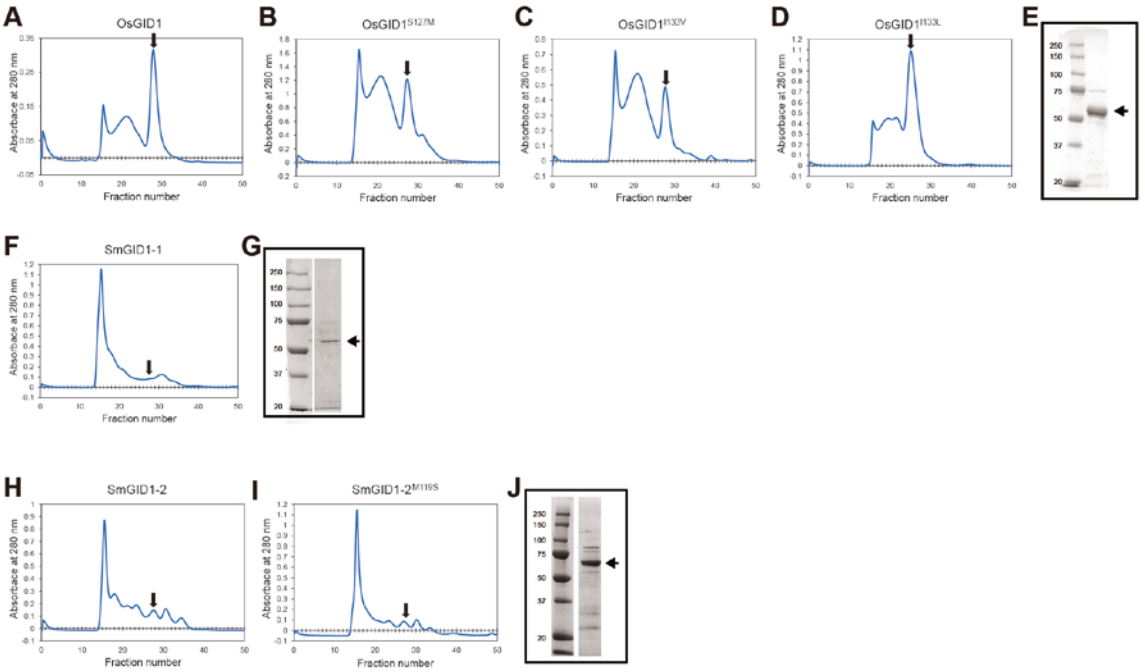

Fig. S5. Gel filtration profiles of the various GID1s used for the binding affinity experiment presented in Fig. 2c. (*A–D*), OsGID1 and its variants. (*E*) SDS-PAGE profile of OsGID1. (*F, G*) SmGID1-1 and its SDS-PAGE profile of SmGID1-1. (*H–J*) SmGID1-2, its variant and SDS-PAGE profile of SmGID1-2. Arrows in the gel filtration profiles indicate the peak positions of GID1s, which were used for the SDS-PAGE and binding affinity experiments. Numbers in the SDS-PAGE profile indicate kDa.

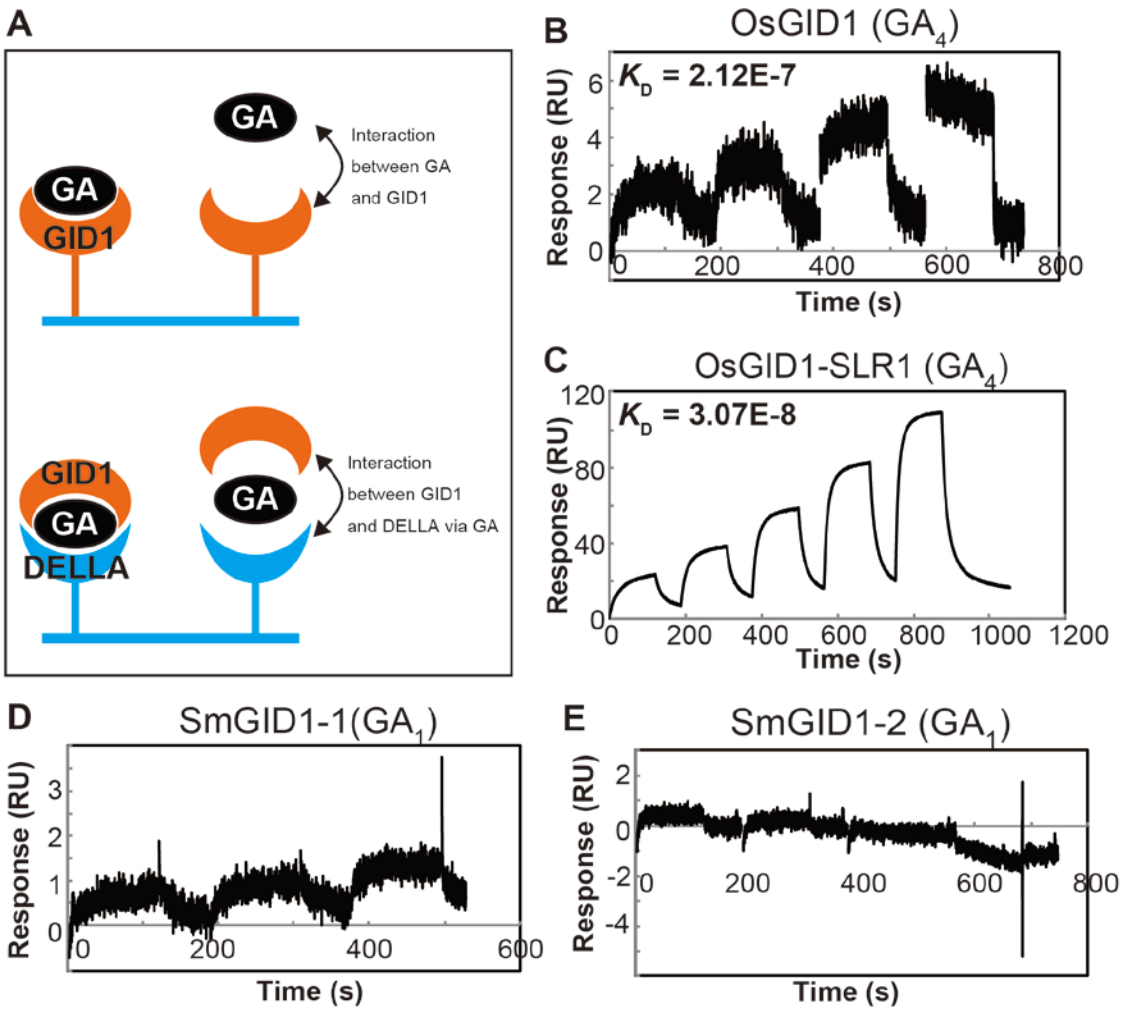

Fig. S6. Effect of K_D of GAs to GID1s through the measurement of the DELLA–GID1 interaction at various GA concentrations under excess GID1 and DELLA by SPR. (*A*) Schematic diagram of SPR analysis to evaluate the GA–GID1 interaction by direct interaction between GA and GID1 without DELLA protein (upper) or by interaction between GID1 and DELLA via GA (lower). (*B*, *C*) Sensorgrams of SPR for GA_4–OsGID1 interaction estimated by the direct method without SLR1 (*B*), or by indirect method estimated by OsGID1–SLR1 interaction via GA_4 (*C*). Binding affinity (K_D) estimated by the indirect method was 6.9 times higher than that by the direct method (2.12E-7 *vs*. 3.07E-8), with a more reliable sensorgram. (*D*, *E*) Sensorgrams of GA_1–SmGID1-1 (*D*) and GA_1–SmGID1-2 (*E*) interaction by the direct method. Binding affinities of GA_1–SmGID1-1 and GA_1–SmGID1-2 could hardly or not be estimated by the direct method.

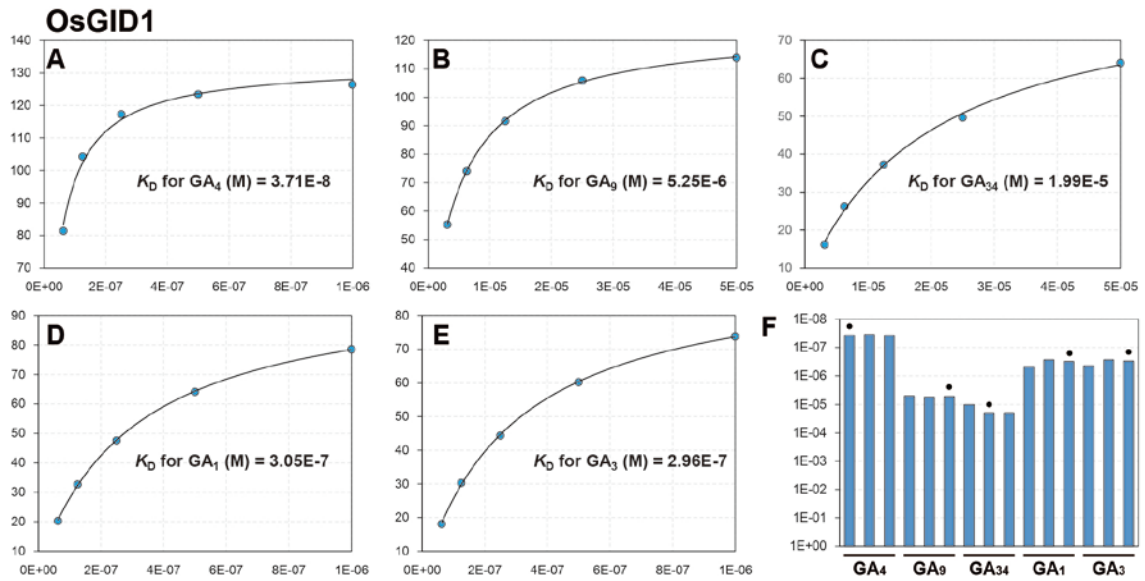

Fig. S7. Estimation of OsGID1–GA interaction affinities. (*A–E*), Equilibrium curves of the OsGID1–SLR1 interaction at various concentration of GA_4 (*A*), GA_9 (*B*), GA_{34} (*C*), GA_1 (*D*), and GA_3 (*E*). K_D was estimated by fitting equilibrium-binding data using a one-site-specific binding model. **f**, We performed three experiments for each GID1–GA combination to calculate the K_D value and adopted the median value as the representative one shown in Fig. 2*C*.

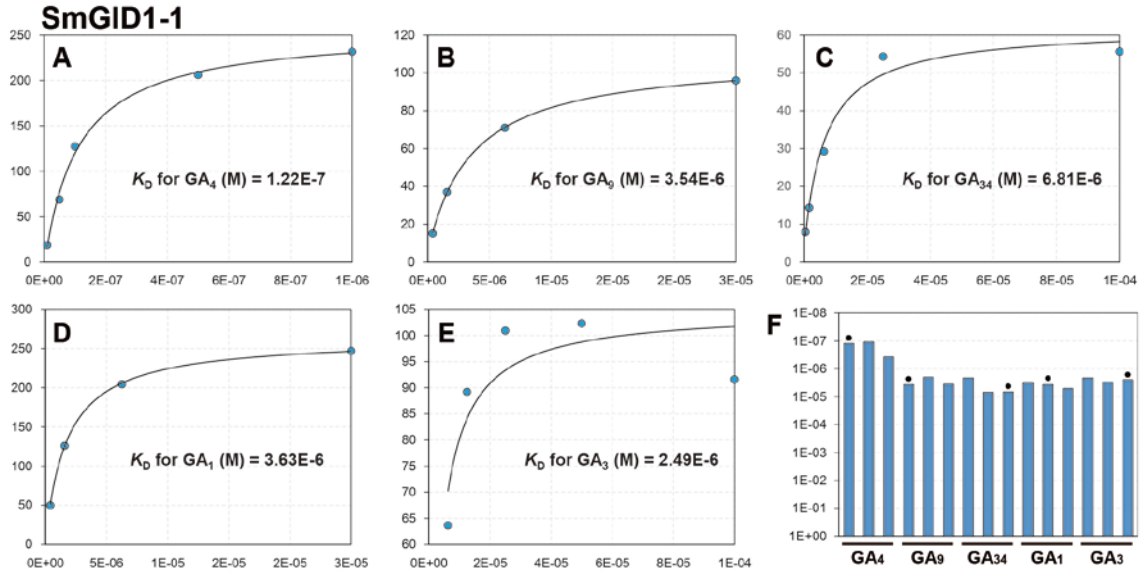

Fig. S8. Estimation of the SmGID1-1–SmDELLA1 interaction affinity. Experimental conditions are the same as in *SI Appendix*, Fig. S7.

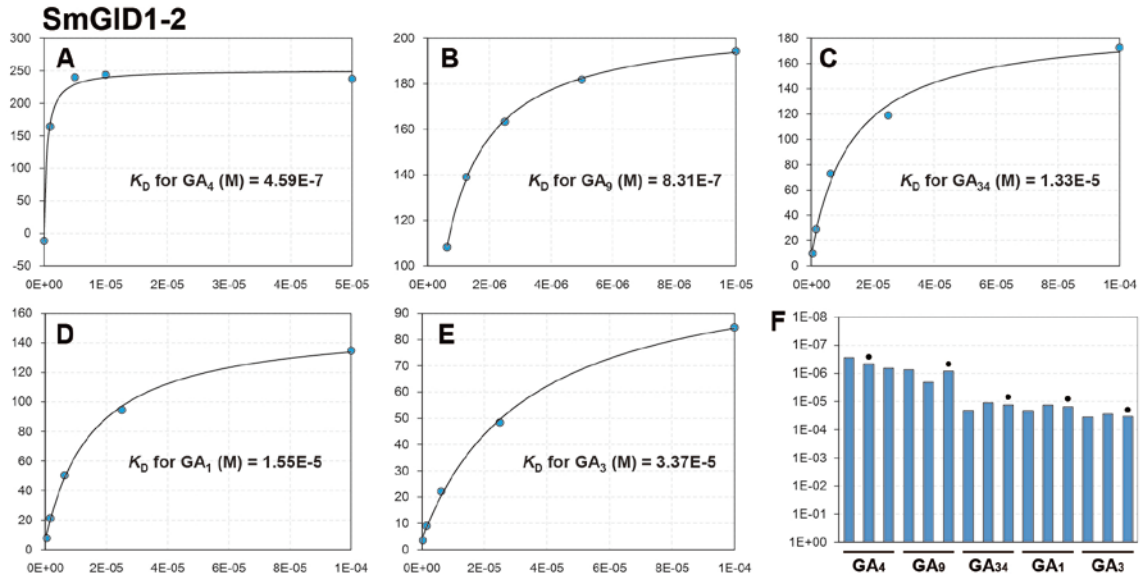

Fig. S9. Estimation of the SmGID1-2–SmDELLA1 interaction affinity. Experimental conditions are the same as in *SI Appendix*, Fig. S7.

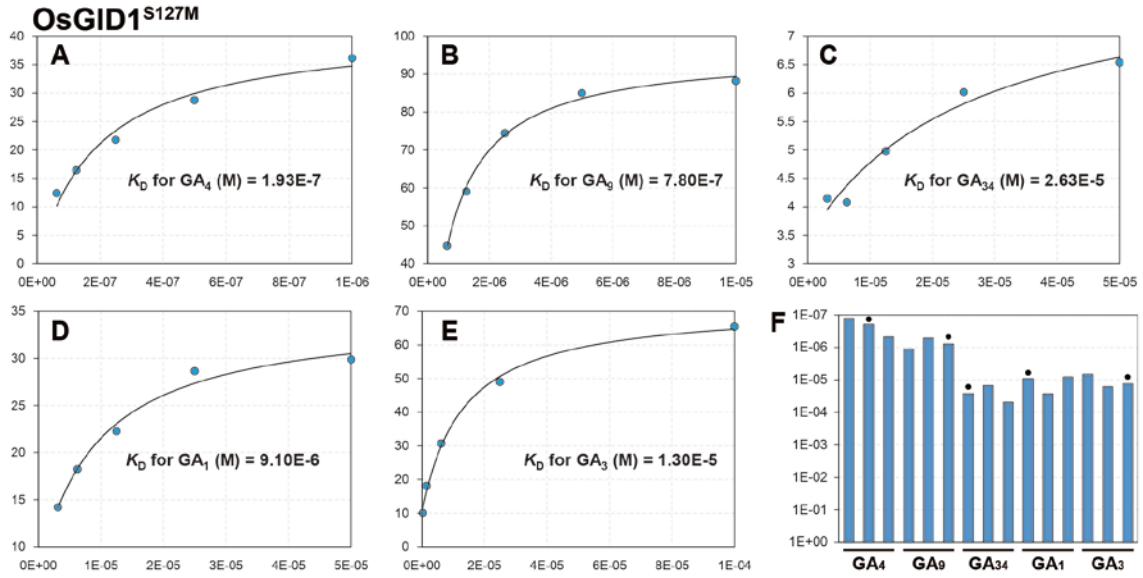

Fig. S10. Estimation of the OsGID1^{S127M}–SLR1 interaction affinity. Experimental conditions are the same as in *SI Appendix*, Fig. S7.

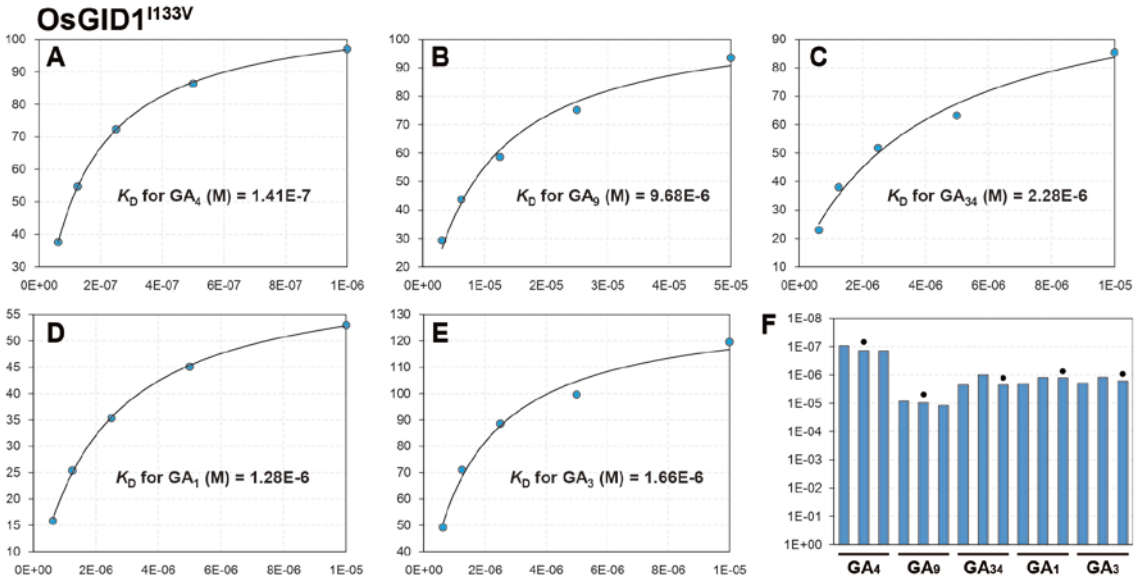

Fig. S11 Estimation of the OsGID1^{I133V}–SLR1 interaction affinity. Experimental conditions are the same as in *SI Appendix*, Fig. S7.

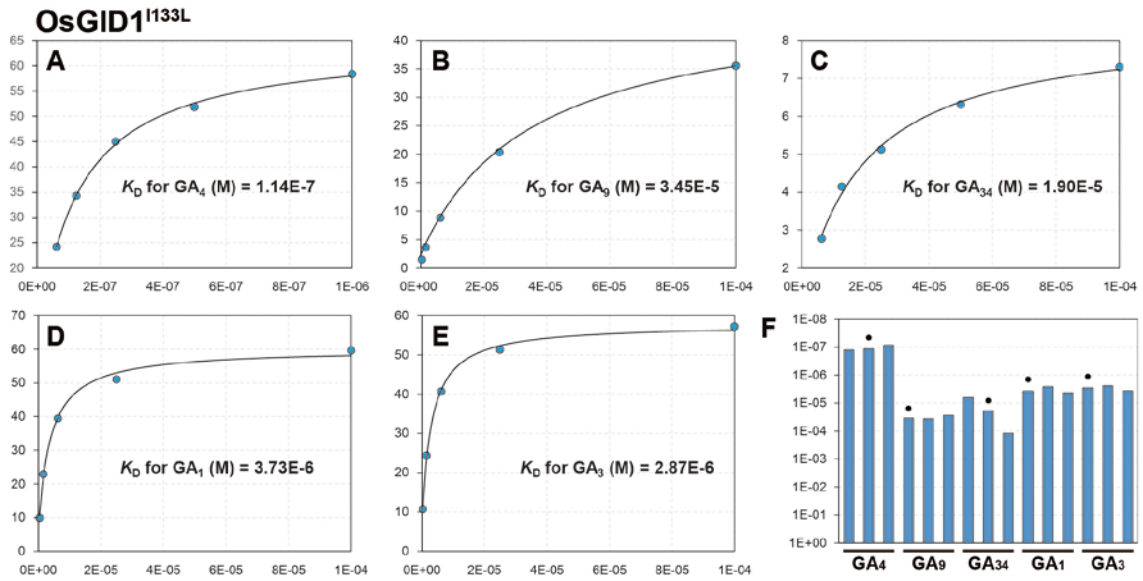

Fig. S12. Estimation of the OsGID1^{I133L}–SLR1 interaction affinity. Experimental conditions are the same as in *SI Appendix*, Fig. S7.

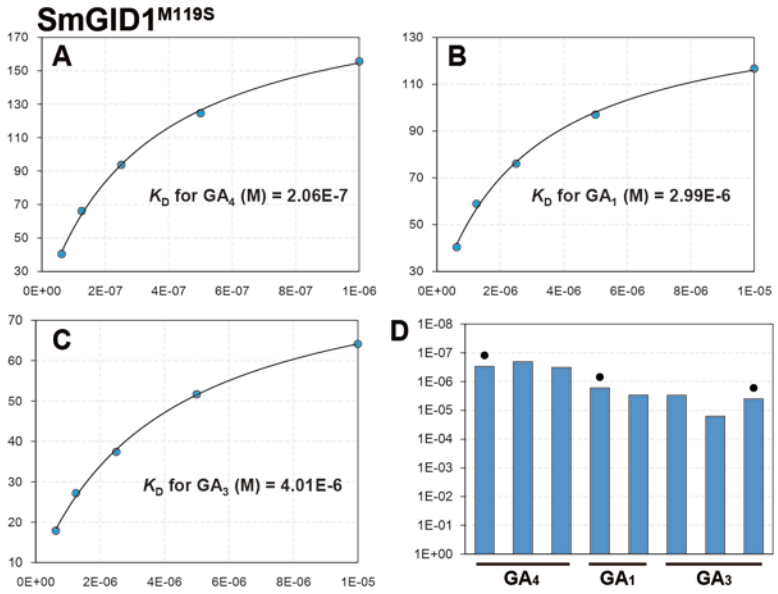

Fig. S13. Estimation of the SmGID1-2^{M119S}–SmDELLA1 interaction affinity. Experimental conditions, but not the analyzed GAs, are the same as in *SI Appendix*, Fig. S7.

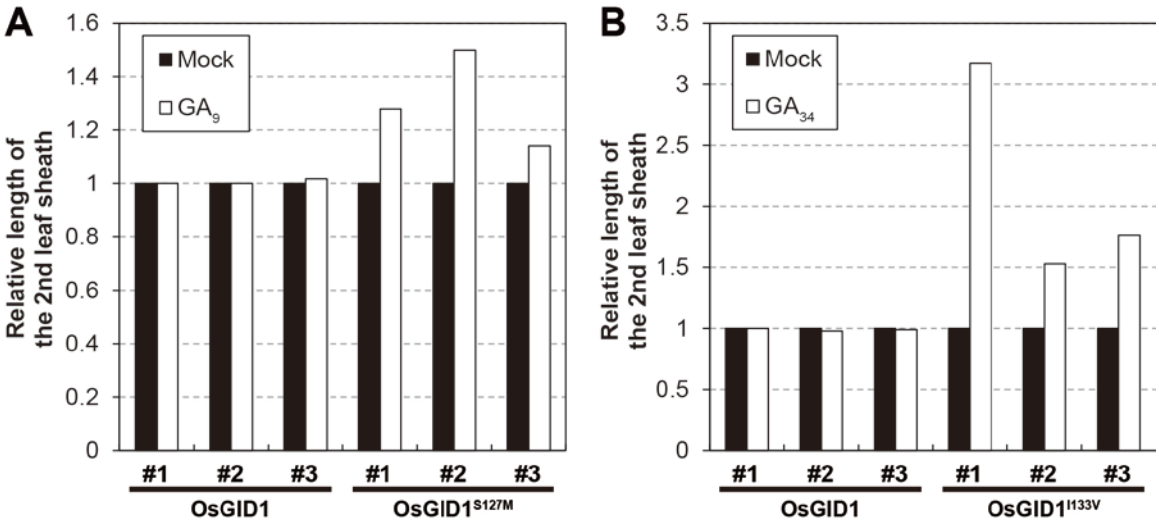

Fig. S14. Comparative length of the 2nd leaf sheath in rice *gid1* null plants overexpressing WT-OsGID1, OsGID1^{S127M}, or OsGID1^{I133V} grown in the presence or absence of 10^{-6} M of GA_9 or GA_{34}. Two plants derived from the same callus were treated, and the leaf sheath length of mock-treated plants was set to 1.

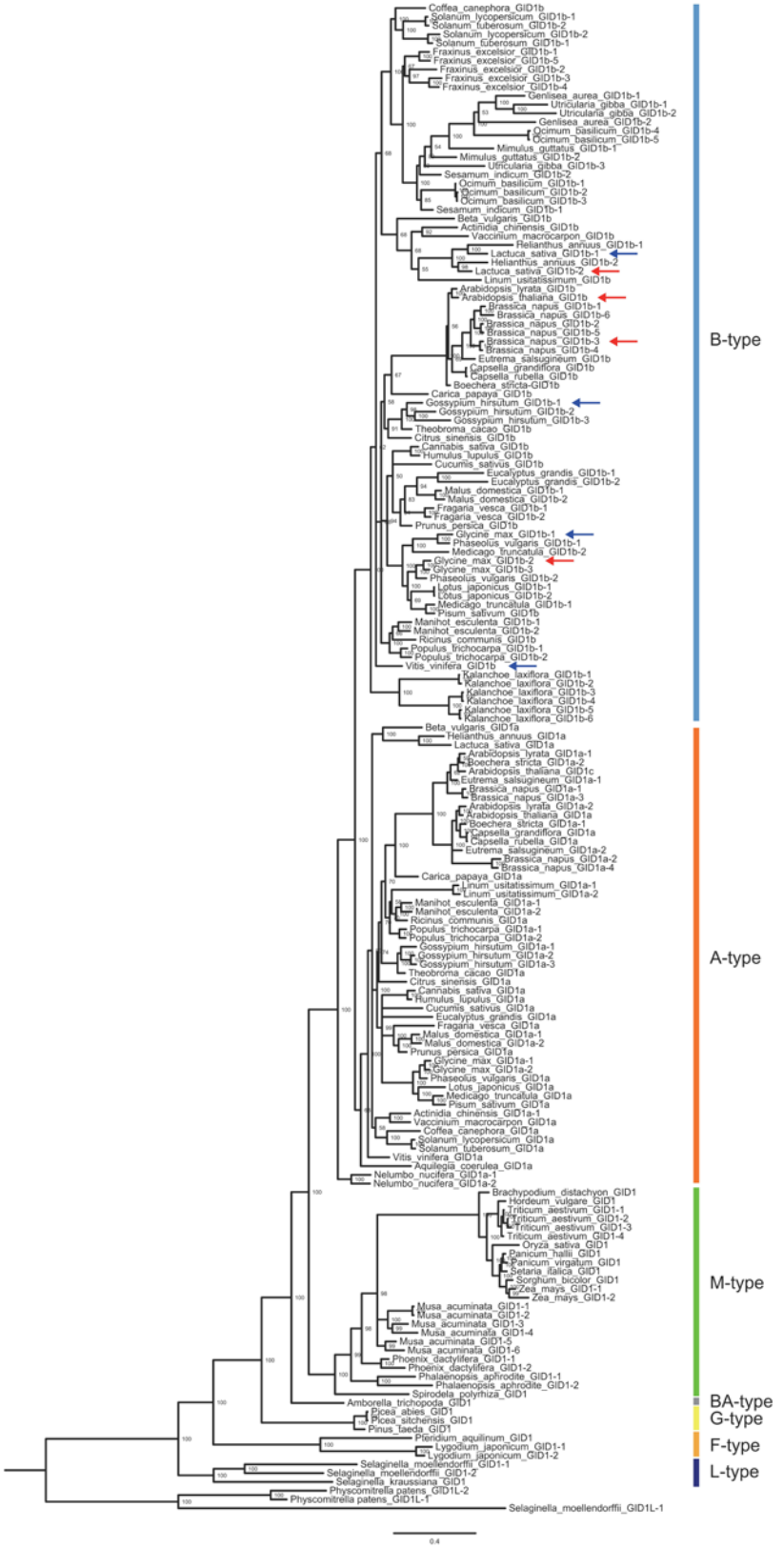
B-type
A-type
M-type
BA-type
G-type
F-type
L-type
0.4

Fig. S15. Phylogenetic analysis of GID1s based on the alignment presented in *SI Appendix*, Dataset S3. Horizontal branch lengths are proportional to the estimated number of amino acid substitutions per residue. A-type; eudicot GID1s including AtGID1a and 1c. B-type; eudicot GID1s including AtGID1b. M-type; monocot GID1s. BA-type: basal angiosperm GID1. G-type: gymnosperm GID1s. F-type: fern GID1s. L-type: lycophyte GID1s. Branch nodes show posterior probability.

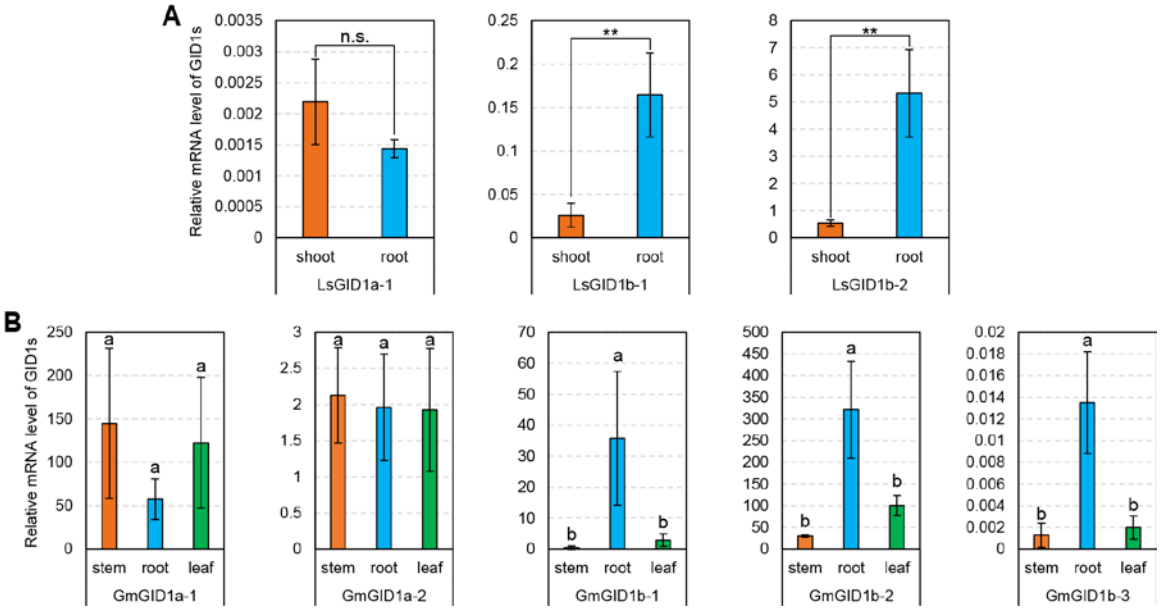

Fig. S16. Expression pattern of *GID1s* in various organs of lettuce (*A*) and soybean (*B*) as estimated by RT-PCR. Lettuce and soybean have one and two A-type GID1s, and two and three B-type GID1s, respectively. $^{**}P < 0.01$ based on two-sided Student's t-test, n.s.; not significant, $P > 0.05$. Different letters indicate significant differences at the 1% level as determined by the Tukey–Kramer test.

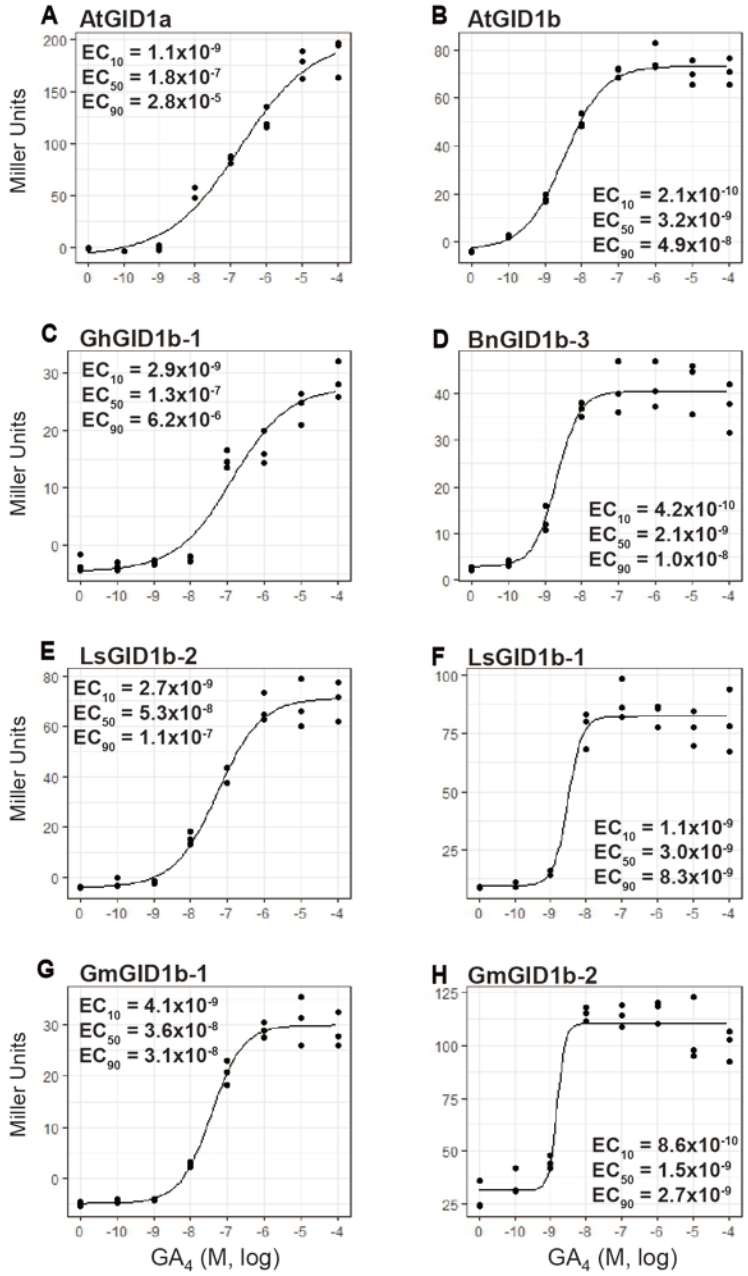

Fig. S17. Quantitative β-galactosidase assay for GA_4 dose-dependence of the interactions of various eudicot GID1s with *A. thaliana* GAI in Y2H. (*A*) AtGID1a was used as a bait. (*B*) AtGID1b. (*C*) GhGID1b-1. (*D*) BnGID1b-3. (*E*) LsGID1b-2. (*F*) LsGID1b-1. (*G*) GmGID1b-1. (*H*) GmGID1b-2. Activity of β-galactosidase was quantified in terms of Miller Units by liquid assay. The 10%, 50%, and 90% of the maximum effective concentration of GA_4 (EC_{10}, EC_{50}, EC_{90}, molar) are shown in the graph. n=3.

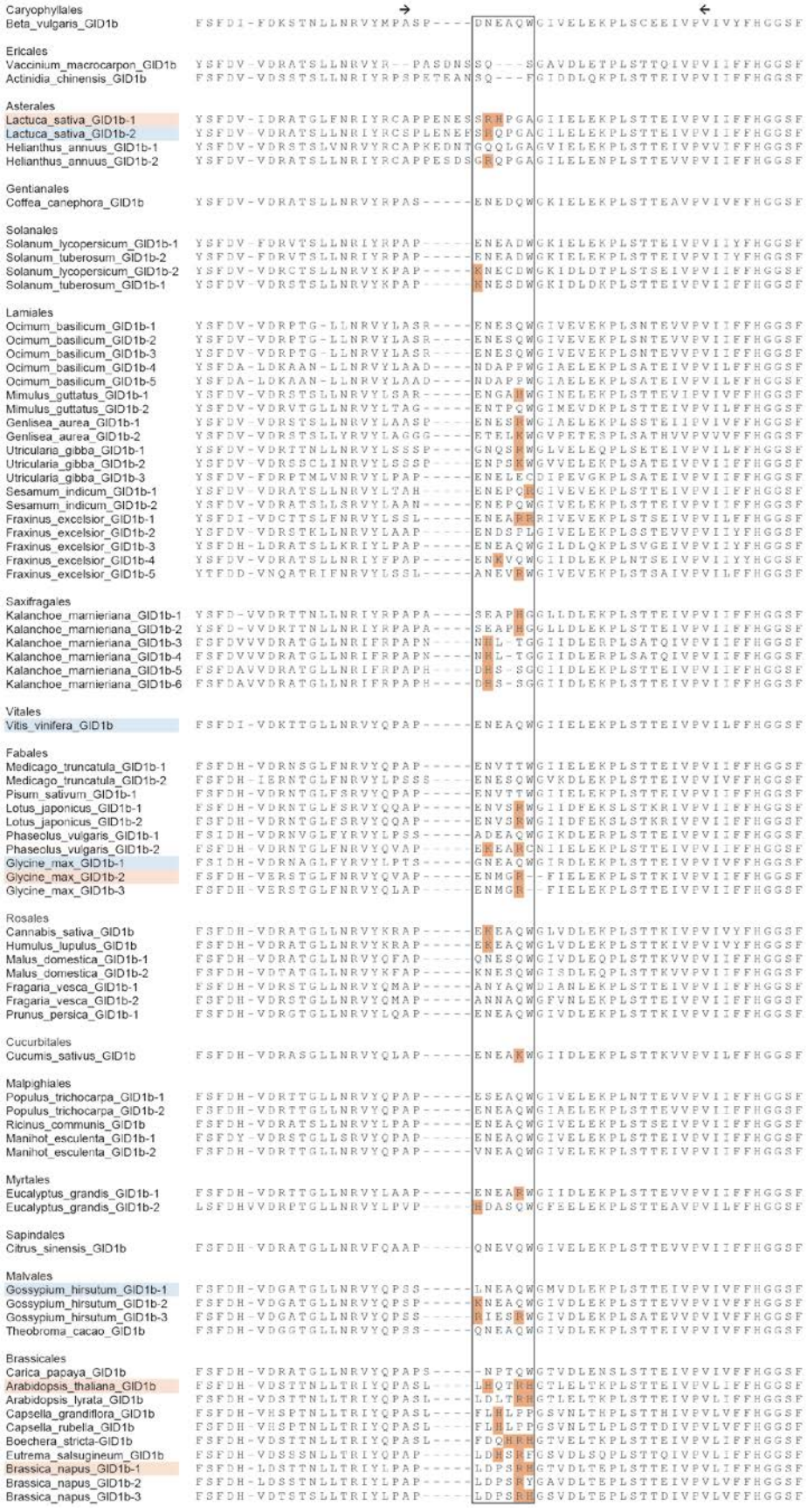
Caryophyllales
Beta_vulgaris_GID1b
Ericales
Vaccinium_macrocarpon_GID1b
Actinidia_chinensis_GID1b
Asterales
Lactuca_sativa_GID1b-1
Lactuca_sativa_GID1b-2
Helianthus_annuus_GID1b-1
Helianthus_annuus_GID1b-2
Gentianales
Coffea_canephora_GID1b
Solanales
Solanum_lycopersicum_GID1b-1
Solanum_tuberosum_GID1b-2
Solanum_lycopersicum_GID1b-2
Solanum_tuberosum_GID1b-1
Lamiales
Ocimum_basilicum_GID1b-1
Ocimum_basilicum_GID1b-2
Ocimum_basilicum_GID1b-3
Ocimum_basilicum_GID1b-4
Ocimum_basilicum_GID1b-5
Mimulus_guttatus_GID1b-1
Mimulus_guttatus_GID1b-2
Genlisea_aurea_GID1b-1
Genlisea_aurea_GID1b-2
Utricularia_gibba_GID1b-1
Utricularia_gibba_GID1b-2
Utricularia_gibba_GID1b-3
Sesamum_indicum_GID1b-1
Sesamum_indicum_GID1b-2
Fraxinus_excelsior_GID1b-1
Fraxinus_excelsior_GID1b-2
Fraxinus_excelsior_GID1b-3
Fraxinus_excelsior_GID1b-4
Fraxinus_excelsior_GID1b-5
Saxifragales
Kalanchoe_marnieriana_GID1b-1
Kalanchoe_marnieriana_GID1b-2
Kalanchoe_marnieriana_GID1b-3
Kalanchoe_marnieriana_GID1b-4
Kalanchoe_marnieriana_GID1b-5
Kalanchoe_marnieriana_GID1b-6
Vitales
Vitis_vinifera_GID1b
Fabales
Medicago_truncatula_GID1b-1
Medicago_truncatula_GID1b-2
Pisum_sativum_GID1b-1
Lotus_japonicus_GID1b-1
Lotus_japonicus_GID1b-2
Phaseolus_vulgaris_GID1b-1
Phaseolus_vulgaris_GID1b-2
Glycine_max_GID1b-1
Glycine_max_GID1b-2
Glycine_max_GID1b-3
Rosales
Cannabis_sativa_GID1b
Humulus_lupulus_GID1b
Malus_domestica_GID1b-1
Malus_domestica_GID1b-2
Fragaria_vesca_GID1b-1
Fragaria_vesca_GID1b-2
Prunus_persica_GID1b-1
Cucurbitales
Cucumis_sativus_GID1b
Malpighiales
Populus_trichocarpa_GID1b-1
Populus_trichocarpa_GID1b-2
Ricinus_communis_GID1b
Manihot_esculenta_GID1b-1
Manihot_esculenta_GID1b-2
Myrtales
Eucalyptus_grandis_GID1b-1
Eucalyptus_grandis_GID1b-2
Sapindales
Citrus_sinensis_GID1b
Malvales
Gossypium_hirsutum_GID1b-1
Gossypium_hirsutum_GID1b-2
Gossypium_hirsutum_GID1b-3
Theobroma_cacao_GID1b
Brassicales
Carica_papaya_GID1b
Arabidopsis_thaliana_GID1b
Arabidopsis_lyrata_GID1b
Capsella_grandiflora_GID1b
Capsella_rubella_GID1b
Boechera_stricta-GID1b
Eutrema_salsugineum_GID1b
Brassica_napus_GID1b-1
Brassica_napus_GID1b-2
Brassica_napus_GID1b-3

Fig. S18. Alignment of the loop regions of β2 and β3 of B-type GID1s. The loop region is indicated between the horizontal arrows at the top. The black box indicates the most variable region. Basic amino acids (Arg and His) in the region are indicated in red. Hypersensitive and normal B-type GID1s, which are evaluated in Fig. 3*C–K*, are indicated in pink and blue, respectively.

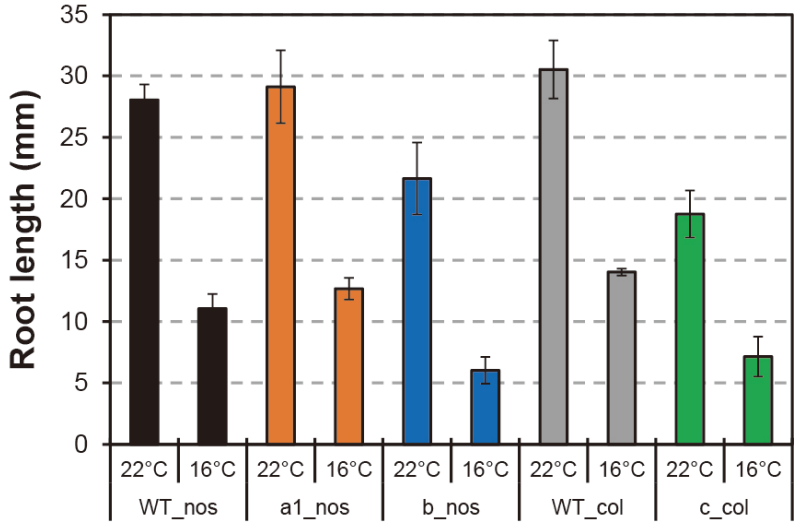

Fig. S19. Effect of low temperature on *A. thaliana gid1* root elongation. Relative root lengths are shown in Fig. 5*F*.

Table S1. Branch models of B-type GID1s. ω, dN/dS rations for clades indicated in Fig. 4*A*.

Model	Hypothesis	ω_0	ω_L	ω_K	ω_B
One	$\omega_0=\omega_L=\omega_K=\omega_B$	0.079	$=\omega_0$	$=\omega_0$	$=\omega_0$
Two	$\omega_0\neq\omega_L$	0.07522	0.103	$=\omega_0$	$=\omega_0$
Two'	$\omega_0\neq\omega_K$	0.0789	$=\omega_0$	0.107	$=\omega_0$
Three	$\omega_0\neq\omega_L\neq\omega_B$	0.07254	0.103	$=\omega_0$	0.161

Table S2. Likelihood ratio tests of branch models. Four branch models shown in *SI Appendix*, Table S1 were compared. df, degrees of freedom; 2ΔlnL, likelihood ratio test statistic.

Model	Null model	df	2ΔlnL	p-value
Two: $\omega_0\neq\omega_L$	One: $\omega_0=\omega_L=\omega_K=\omega_B$	1	7.632007	9.3481E-05
Two': $\omega_0\neq\omega_K$	One: $\omega_0=\omega_L=\omega_K=\omega_B$	1	0.258187	0.47239254
Three: $\omega_0\neq\omega_L\neq\omega_B$	Two: $\omega_0\neq\omega_L$	1	15.277529	3.2452E-08

Four branch models shown in *SI Appendix*, Table S1 were compared. df, degrees of freedom; 2ΔlnL, likelihood ratio test statistic.

Table S3. Primers used in the present study.

Primer name	Sequence
Construction for rice transformation	
mGID1-Y329F	GCCACGGTGGGGTTCGCCCTGTTGCCCAAC
mGID1-Y329R	GTTGGGCAACAGGGCGAACCCCACCGTGG C
mGID1-N225F	GGCAACATCCTGCTCGCCGCCATGTTCGGC
mGID1-N225R	GCCGAACATGGCGGCGAGCAGGATGTTGC C
mGID1-S198F	CTCTCCGGCGACGCCTCCGGCGGCAACATC
mGID1-S198R	GATGTTGCCGCCGGAGGCGTCGCCGGAGA G
mGID1-S123F	CTTCCACGGCGGCGCCTTCGTGCACTCGTC
mGID1-S123R	GACGAGTGCACGAAGGCGCCGCCGTGGAA G
mGID1-R251F	GTGACGCTCCAGGACGCGGACTGGTACTG G
mGID1-R251R	CCAGTACCAGTCCGCGTCCTGGAGCGTCAC
mGID1-D250F	CGTGACGCTCCAGGCCAGGGACTGGTACTG
mGID1-D250R	CAGTACCAGTCCCTGGCCTGGAGCGTCACG
mGID1-Y134F	GCCAGCTCGACCATCGCCGACAGTCTGTGC
mGID1-Y134R	GCACAGACTGTCGGCGATGGTCGAGCTGG C
mGID1-S127F	GGCAGCTTCGTGCACGCGTCGGCCAGCTC G
mGID1-S127R	CGAGCTGGCCGACGCGTGCACGAAGCTGC C
mGID1-Y31F	CTTCAAGCTGTCGGCCAACATTCTGCGGCG
mGID1-Y31R	CGCCGCAGAATGTTGGCCGACAGCTTGAAG
mGID1-I133F	GGCCAGCTCGACCGCCTACGACAGTCTGTG
mGID1-I133R	CACAGACTGTCGTAGGCGGTCGAGCTGGCC
mGID1-L330F	CGGTGGGGTTCTACGCGTTGCCCAACACCG
mGID1-L330R	CGGTGTTGGGCAACGCGTAGAACCCCACCG
mGID1-F27F	GTGCTCATCTCCAACGCCAAGCTGTCGTAC
mGID1-F27R	GTACGACAGCTTGGCGTTGGAGATGAGCAC

mGID1-V326F	GAGAACGCCACGGCGGGGTTCTACCTGTTG
mGID1-V326R	CAACAGGTAGAACCCCGCCGTGGCGTTCTC
mGID1-I24F	CACACATGGGTGCTCGCCTCCAACTTCAAG
mGID1-I24R	CTTGAAGTTGGAGGCGAGCACCCATGTGTG
mGID1-F245F	CTCGACGGCAAGTACGCCGTGACGCTCCAG
mGID1-F245R	CTGGAGCGTCACGGCGTACTTGCCGTCGAG
mGID1-V246F	GGCAAGTACTTCGCGACGCTCCAGGACAGG
mGID1-V246R	CCTGTCCTGGAGCGTCGCGAAGTACTTGCC
mGID1-Y254F	CAGGACAGGGACTGGGCCTGGAAGGCGTAC
mGID1-Y254R	GTACGCCTTCCAGGCCCAGTCCCTGTCCTG
GID1-I133V-F	GGCCAGCTCGACCGTCTACGACAGTCTGTG
GID1-I133V-R	CACAGACTGTCGTAGACGGTCGAGCTGGCC
Construction for yeast assays	
EcoRI+VvGID1b.F	GGAATTCATGGCCGGGAGTGATGAAGT
PAPEN+GmGID1-2.loop.R	CTCTATGAACCTTCCCATATTTTCAGGCGCAGG
GmGID1-2.loop+LEKPL	ATGGGAAGGTTCATAGAGCTGGAAAAGCCCTTG
VvGID1b.R+BamHI	CGGGATCCTTAACAGTTAGATTTCACGA
Construction for protein expression in *E. coli*	
GID1-S127M-F	CAGCTTCGTGCACATGTCGGCCAGCTCGAC
GID1-S127M-R	GTCGAGCTGGCCGACATGTGCACGAAGCTG
GID1-I133L-F	GGCCAGCTCGACCCTCTACGACAGTCTGTG
GID1-I133L-R	CACAGACTGTCGTAGAGGGTCGAGCTGGCC
GID1-I133V-F	GGCCAGCTCGACCGTCTACGACAGTCTGTG
GID1-I133V-R	CACAGACTGTCGTAGACGGTCGAGCTGGCC
BamHI+SmDELLA1(14K125S).F	GCGGATCCAAGAGCCGGATGATCCCGGTAG
SmDELLA1(14K125S)+EcoRI.R	GCGAATTCCGATTCCATATCGGAGGACGAG
BamHI+SmDELLA1.F	GCGGATCCATGGAGGATATGGATATGCTCG
SmaI+T+SmGID1a.F	GCCCCGGGTATGAATTCCTGTAGCAAG
SmaI+T+SmGID1b.F	GGCCCGGGTATGGAACCGGAGGAGGAT

	SmGID1a.R+SalI	GCGTCGACTCACGTCGAGGAATCCATG
	SmGID1b.R+SalI	GCGTCGACCTACGTTGTTGTCCTGCGA
	SmGID1bM120S.f	CAGCTTCGTGCACTCGTCCGCTAACAGTGC
	SmGID1bM120S.r	GCACTGTTAGCGGACGAGTGCACGAAGCTG
qRT-PCR		
	Ls.Ubiquitin-protein.F	TCTTAGATCACCGTCCCATCGT
	Ls.Ubiquitin-protein.R	TCTGAGATTGTCCGAGGATATGAG
	LsGID1a.RT1.F	CCAAATTAACGTCTGCGAATC
	LsGID1a.RT1.R	GCCGGAGAAGGTTGTAAGC
	LsGID1bc.RT1.2.F	AAGCAGGGCAAGACGTGAAG
	LsGID1bc.RT1.3.R	GCGAGACTCAACGAACAAACC
	LsGID1ac.RT1.F	TAGTGGTGGTGGCCGGATTAG
	LsGID1ac.RT1.3.R	ACTTGTTGCCCTGCGTTTTC
	GmRPL30.RT.F	CAATGCTGCACTTAATTTTTGCCG
	GmRPL30.RT.R	GAAGAACACATCATTCACATTAAT
	GmGID1a-1.RT2.F	CATTCCTATGTCTTGGGTTGG
	GmGID1a-1.RT2.R	AACATTGCTGCGGAAAAGAC
	GmGID1a-2.RT1.F	ACGACAAGTGGGCGTTAGAA
	GmGID1a-2.RT1.R	AATAGCGGGAGCAAAGTCCT
	GmGID1b-1.RT1.F	CTGGGGACTACTGCTTCCTG
	GmGID1b-1.RT1.R	CCCAAATGAACCGAGTTCTG
	GmGID1b-2.RT2.F	TGGCTGAAGCAACGTAAATG
	GmGID1b-2.RT2.R	AAGCGATAAGCCAAGCCATA
	GmGID1b-3.RT1.F	CTTCCTGTGCTGTGCTCAAA
	GmGID1b-3.RT1.R	CTTCAGCCAAACCCCACTAA

Dataset S1.

Amino acid alignment of GID1s and GID1-like CXEs for the phylogenetic analysis presented in *SI Appendix*, Fig. S1. GID1s or GID1-like CXEs in clade IV are indicated in red and grey, respectively, whereas five GID1-like CXEs used for the alignment in *SI Appendix*, Fig. S2 are marked by red dots. Six non-polar amino acids of OsGID1 replaced with Ala or Ser in *SI Appendix*, Fig. S4 and the corresponding residues of GID1-like CXEs are indicated in red. Y134 of OsGID1 and the corresponding residues of GID1-like CXEs are indicated in yellow.

Dataset S2.

CXE and *GID1* genes used in the present study.

Dataset S3.

Amino acid alignment of 169 GID1s from various plant species for the phylogenetic analysis presented in *SI Appendix*, Fig. S15.

Dataset S4.

Amino acid alignment of 83 B-type GID1s for the phylogenetic analysis presented in Fig. 4*A*.